Absolute Rate Constants for Collisional Vibrational Relaxation in Dense Vibrational Regions of S_1 *p*-Difluorobenzene†

Todd A. Stone‡ and Charles S. Parmenter*

Department of Chemistry, Indiana University, Bloomington, Indiana 47405

Received: June 5, 2001; In Final Form: October 16, 2001

To gain insight into the possible magnitude of vibrational activation/deactivation rate constants for large molecules with the high vibrational excitation of thermal unimolecular reactions, absolute vibrational relaxation rate constants have been measured in S_1 *p*-difluorobenzene energy regions where the vibrational levels begin to form a quasi-continuum. The measured rate constants define vibrational energy transfer from three initially pumped S_1 levels into the surrounding vibrational field. The observed rate constants are about 60% of the Lennard-Jones value for the collision partner Ar and about 40% for He. The initial levels lie in the ϵ_{vib} range 2887 to 3310 cm^{-1}, where the level densities are approximately 800−2000 per cm^{-1}. New He rate constants are also measured for many lower initial levels. When combined with earlier measurements, the He and Ar rate constants span the range $0 \leq \epsilon_{vib} \leq 3310$ cm^{-1}. Both sets of rate constants show a trend to larger values with increasing ϵ_{vib} and have prominent variations in response to the zero order quantum identity of the initial level. When the high level density starts to create overlapping states, the Ar rate constants for the three highest levels appear to have leveled off, and the initial quantum state variations are damped out. The He rate constants, on the other hand, sustain the trend to larger values even at the highest energies where the data are ambiguous on whether initial quantum state sensitivity persists.

Introduction

This study concerns the destruction of a vibrational state in a large molecule by collisional energy transfer into the surrounding vibrational field, a process we shall call state-to-field vibrational energy transfer (VET). The study is a continuation of efforts to measure absolute rate constants for this VET from regions of increasingly high state densities in large molecules. Previous studies with benzene[1,2] and with *p*-difluorobenzene (pDFB)[3−5] in collision with rare gases or diatomic molecules have characterized the state-to-field rate constants for vibrational levels ranging from the zero point level to regions where the vibrational level densities reach, in the case of pDFB, several hundred per cm^{-1}. Here, we describe extension of the pDFB study for both He and Ar collision partners to three higher levels where the vibrational state density climbs by about an order of magnitude. The extension is significant because the highest levels now get into regions where the vibrational states begin to form a quasi-continuum by level overlap.

Our motivation is derived from work on the collisional activation and deactivation of molecules with the high internal energy associated with thermal unimolecular reactions. Since this energy is principally vibrational, the collisions of interest are those between an excited molecule and, e.g., a bath gas molecule that causes change in the vibrational excitation. These collisional processes have long remained under active study,[6−11] and we shall refer to their study as the activation/deactivation problem.

Much progress has been made toward characterizing the average vibrational energy change in such collisions as well as in defining the probability distribution $P(E',E)$ that a molecule with initial energy E' will finish the collision with vibrational energy in the range $E + dE$. Such modeling requires factorization of the energy transfer into probability *per collision* with the use of an absolute rate constant whose value defines a collision for the energy change. None, however, has ever been measured for these regions where the vibrational state density is so high that a vibrational quasi-continuum is present. A method to do so has not been devised, and in the absence of experimental data, Lennard-Jones rate constants are generally assumed for the modeling.[12−25]

It is useful to learn experimentally about the validity of the Lennard-Jones assumption. Our previous state-to-field VET measurements may help one do this since they involve processes analogous to those of the activation/deactivation problem. In both cases, collision causes a molecule with an initial vibrational energy ϵ_{vib} to gain or lose vibrational energy into the surrounding vibrational field. Our indirect approach to learning about the magnitude of the VET rate constant for the vibrational quasi-continuum region of a large molecule with high excitation is to measure absolute state-to-field VET rate constants for a series of initial levels with increasing vibrational energy. By observing the rate constant behavior as the vibrational level density becomes that of an increasingly dense quasi-continuum, one may gain insight into the size of rate constants that pertain to VET in the high energy regions of unimolecular activation.

The present work builds on the previous study by Catlett, Pursell and Parmenter[4] (CPP) that used vibrational structure in the S_1-S_0 fluorescence to measure rate constants for state-to-field VET in S_1 pDFB in collision with Ar for 18 initially pumped levels. Those levels ranged from the zero-point level to $\epsilon_{vib} = 2502$ cm^{-1}. Higher levels were not accessible because

† This paper was submitted for the Edward W. Schlag Festschrift, published as the June 14, 2001, issue of *J. Phys. Chem. A.*

* To whom correspondence should be addressed. E-mail: parment@indiana.edu. Fax: (812) 855-8300.

‡ Present address: Department of Chemistry and Chemical Biology, Harvard University, 12 Oxford Street, Cambridge, Massachusetts 02138.

10.1021/jp0121365 CCC: $22.00
Published on Web 01/18/2002

changes in the fluorescence spectrum made the signal-to-noise too small for quantitative measurements.

Improved spectroscopic techniques now allow us to explore three higher S_1 vibrational regions where the level density is in the range 800−2000 per cm^{-1}. This extension is important because it gives access to regions where the vibrational levels just begin to overlap and form a quasi-continuum. These regions are now studied with the collision partner Ar to extend the Ar rate constant data of CPP. Additionally, He state-to-field rate constants have been obtained for many S_1 levels ranging from $\epsilon_{vib} = 800$ cm^{-1} to the highest level of the new Ar study. Data for He were not previously available for any of these levels.

The method by which the state-to-field VET rate constants are measured[4] involves preparation of an S_1 level or, more accurately, a narrow S_1 vibrational region by pumping a band maximum in the 300 K $S_1 \leftarrow S_0$ pDFB absorption spectrum. A vibrational band from the initially pumped S_1 level is isolated in the fluorescence spectrum and its intensity monitored as a function of added Ar or He. Since the collision-free fluorescence lifetime is known from prior work,[26] the absolute state-to-field VET rate constant can be calculated. It is straightforward to control gas pressures so that added gases are in the single collision regime and that collisions between S_1 and S_0 pDFB molecules do not play a significant role.[4]

It is important to note that this technique enables the state-to-field VET rate constant to be isolated from elastic and other inelastic processes that contribute to a total collision rate constant. Effects of rotational relaxation, for example, are avoided by monitoring the entire vibrational band intensity so that variation in the band contour that accompanies rotational state changes become invisible. Electronic state quenching by Ar and by He is known by separate measurements of total fluorescence intensity[27] to have rate constants that are too small to contribute significantly to the vibrational band measurements. Finally, interference from specific state-to-state VET channels is precluded by choosing the monitored $S_1 \rightarrow S_0$ vibrational band in a spectral region free of emission from the destination states.

There is always concern that rate constants measured for VET processes in an S_1 state may not be representative of those for the ground electronic state. In the case of pDFB, the issue is illuminated by comparing measurements with many collision partners on four S_0 levels[3,5] with the S_1 data of CPP. When the four Ar S_0 values are compared with S_1 values for similar state densities ranging from about 2 to 200 per cm^{-1}, the rate constants are close, never differing by more than a factor of 2. In fact, the S_1 and S_0 rate constants for densities of 10 and 80 states per cm^{-1} match to within 15%.

Much of the background for the present measurements has been given in CPP. Since then, a work bearing on the issue of absolute rate constants for state destruction in molecules with high vibrational energy has appeared.[28] It concerns a single rovibrational level in SO_2 with over 44800 cm^{-1} of vibrational energy whose collisional destruction was monitored with use of quantum beat spectroscopy. The reported rate constants for the collision partners He, Ar and unexcited SO_2 all substantially exceed Lennard-Jones values. As will be shown, these rate constants are much larger than those for the highest pDFB levels, and some comments concerning the differences will be given.

Experimental Procedures

The apparatus and procedures used in the experiments are similar in design to that used for previous studies of pDFB energy transfer.[4] Briefly, gas samples were introduced into a stainless steel cross-shaped fluorescence cell equipped with quartz windows. pDFB pressures of 80 mTorr were used for the lowest vibrational levels. The pDFB pressure increased to as much as 120 mTorr for the highest levels to enable quantitative measurements of a small fluorescence signal. These pressures were still low enough to prevent pDFB-pDFB state changing collisions from occurring within the ∼5 ns fluorescence lifetime. Collision gas pressures up to 5 Torr (representing the single collision regime) were introduced by leaking the gas into the fluorescence cell through a needle valve from a backing pressure usually exceeding 30 Torr. An MKS Baratron 750 absolute pressure transducer monitored the pressure continuously to the nearest mTorr, and the gases were allowed to equilibrate over a 20−30 min period prior to measurements.

The visible output of a Quanta Ray Nd:YAG (DCR 1-A) pumped dye laser (PDL-1) with LDS 698 or DCM dye was frequency doubled and mixed with the residual 1064 nm YAG fundamental, producing tunable UV exciting light with pulse duration of 5 ns at 10 Hz and a bandwidth of 2 cm^{-1}. The laser was tuned to the $S_1 \leftarrow S_0$ absorption maximum of a band contour to prepare initial S_1 levels.

Fluorescence collected orthogonal to the laser beam was imaged into a 0.85 m scanning monochromator operated in second order and detected by an EMI 9789 photomultiplier. The fluorescence was normalized for laser power fluctuations and for pDFB pressure fluctuations by directing four percent of the emission image into a Jobin-Yvon H-20 small monochromator equipped with another photomultiplier that monitored either the laser power or the total fluorescence. Signals from both photomultipliers were processed by a home-built gated detection system. This system improved the signal-to-noise relative to our previous experiments and made study of the higher levels feasible.

Dispersed fluorescence spectra were acquired with 10 cm^{-1} resolution. For VET measurements, the scanning monochromator was tuned to a prominent $S_1 \rightarrow S_0$ emission band to monitor the population of the parent vibrational level as the pressure of the collision partner was increased. Monitored bands were chosen to avoid overlap with emission from collisionally populated levels. These measurements were performed with 40 cm^{-1} fluorescence resolution, a value chosen to be large enough to filter out band broadening effects due to rotational energy transfer but still sufficiently narrow to discriminate against bands arising from collisionally populated levels.

Results and Kinetic Model

We use the kinetic model that was developed in our previous state-to-field studies[2,4] and retain the nomenclature and rate constant numbering scheme. Briefly, a laser pumps pDFB (labeled B) to a specific S_1 vibrational level B**

$$B + h\nu \rightarrow B^{**}$$

which may decay by both radiative ($h\nu_f$) and nonradiative pathways

$$B^{**} \xrightarrow{k_1} B + h\nu_f \quad (1)$$

$$B^{**} \xrightarrow{k_2} \text{nonradiative decay} \quad (2)$$

Vibrational energy transfer via single collisions with the added bath gas (M) or with ground state pDFB molecules (B) may deactivate the initially prepared level by VET into the sur-

rounding S_1 field of vibrational states (B*) with characteristic rate constants.

$$B^{**} + B \xrightarrow{k_3} B^* + B \quad (3)$$

$$B^{**} + M \xrightarrow{k_4} B^* + M \quad (4)$$

Quantitative measurements of selected fluorescence transitions in the dispersed fluorescence spectra of pDFB can be made with pressures so low that collisions with S_0 pDFB destroying the initially prepared state cannot compete measurably with the collision-free S_1 decay. As discussed in earlier work,[27,29] the routine use of low pDFB pressures in our experiments (80−120 mTorr) enables us to ignore process 3. S_1 electronic state quenching by the bath gases has been explored[27] and is negligible in comparison with VET process (4).

The kinetic model gives rise to the standard Stern−Volmer expression for the VET rate constant as a function of added gas,

$$\frac{I_f^0}{I_f^M} = 1 + \frac{k_4}{k_1 + k_2}[M] \quad (5)$$

where I_f^M and I_f^0 are the fluorescence band emission intensities with and without the collision gas, respectively. Thus, a plot of the intensity ratio versus collision gas pressure should be linear with a slope proportional to k_4, the desired quantity. The only quantity needed to extract the VET rate constant from the slope is the collision free fluorescence lifetime of the emitting level, $(k_1 + k_2)^{-1} = \tau_f$. Lifetimes of all levels with the exception of that at 3009 cm^{-1} have been determined.[26] For this level, the lifetime is assumed to be that measured for the 2887 cm^{-1} level lying only 122 cm^{-1} lower in energy.

It is straightforward to tune the dispersed fluorescence spectrometer to an emission band from B** that lies in a region essentially free of emission from the field of S_1 levels B*. In this sense, the experiment may selectively measure the population (via fluorescence intensity) originating from the pumped level without interference arising from collisionally populated S_1 levels.

Figure 1 displays fluorescence excitation spectra of the S_1-S_0 spectral regions used for pumping the three highest levels. The collision-free fluorescence spectra generated by the pumping are shown in Figure 2. In each case, the band monitored for determining the state-to-field VET rate constant has relatively low intensity, but it is so far removed from the dominant unstructured emission region that it can be selectively monitored. The destination levels populated by the state-to-field VET emit in the region of unstructured fluorescence.

Figure 3 shows typical Stern−Volmer plots according to eq 5 for relaxation of these levels by Ar and He. The emission band intensities were typically measured for five pressures of the added gases in order to establish the slope, which was extracted via linear least-squares fitting. Each data point represents an emission band intensity measurement over a span of approximately 10 min. The error bars on each data point result from the standard deviation of the monitored signal over the data collection period. In each case, slopes of at least three separate experiments were averaged to improve the accuracy of the reported rate constants. Uncertainty in the value of the VET rate constant is derived from a standard procedure of calculating the error associated in fitting the slope, and all errors reported in Table 1 are determined from propagation through eq 5 for the average of the three separate trials. In each case,

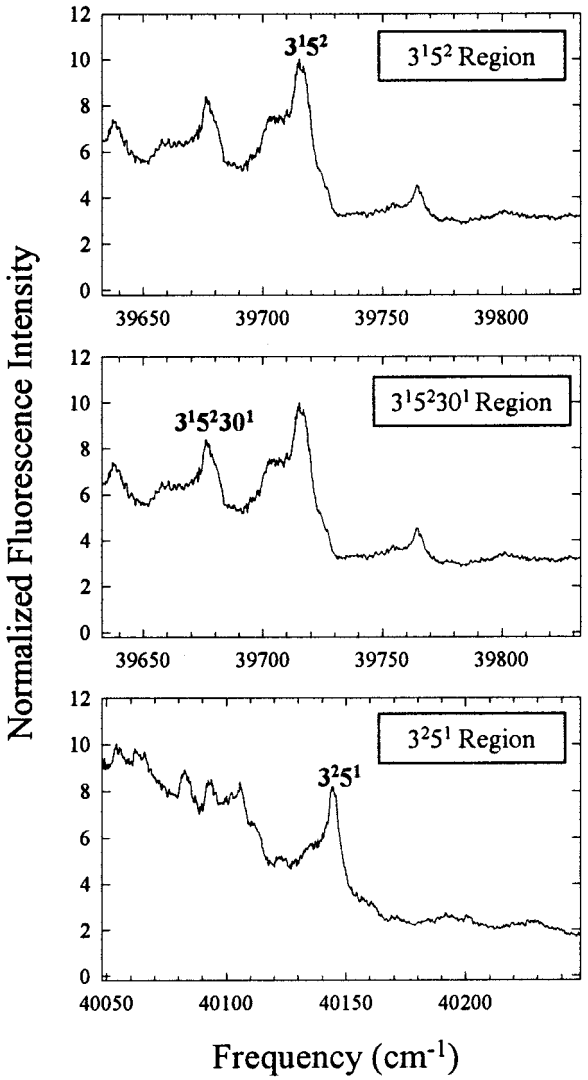

Figure 1. Fluorescence excitation spectra of the areas near the three highest levels pumped for the VET study. The Franck−Condon labels for the S_1 zero-order states are indicated.

the standard error in fitting the slope to the experimental data never exceeded 15−20% of the calculated rate constant value. The reproducibility of the results for individual measurements is judged by the fact that the slopes of repeated experiments fell within 15% of the mean.

Table 1 displays the rate constants so determined for nine S_1 pDFB levels. Those for He are entirely new. While the Ar rate constants for the lower six levels have been previously reported by CPP, the values for those levels shown in Table 1 are from the present revisitation. In each case, the Table 1 value is in reasonable accord with the CPP value, differing in the most extreme case by 17%. The Ar rate constants for the highest three levels have not been previously determined. On the basis of the reproducibility of the experiments, the uncertainty in the k_4 values for all levels and both gases is about 15%.

Discussion

In past studies, the absolute rate constants for state-to field VET have been followed from low state densities up to regions with about 20 states per cm^{-1} for benzene[2] and to about 200 per cm^{-1} for both S_0[3,5] and S_1[4] pDFB. The rate constants trend upward as states of higher initial energy are pumped. In each case, however, the rate constant increase lags far behind that of the state densities, and for S_1 pDFB, the rate constants continue

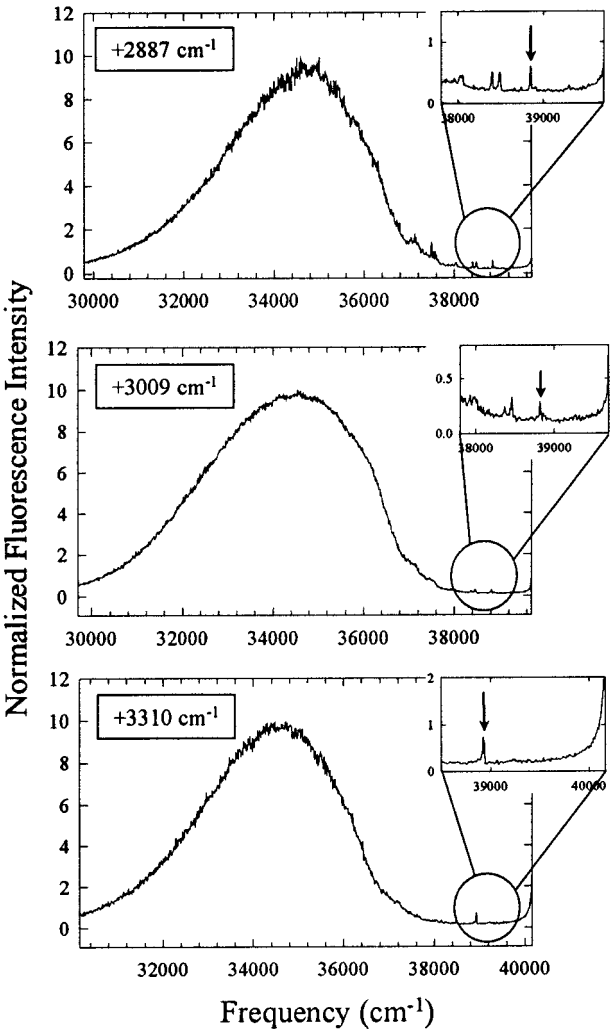

Figure 2. Single vibronic level fluorescence spectra obtained after pumping the maximum of the transitions in Figure 1 to reach +2887, +3009, and +3310 cm^{-1} in vibrational excitation, respectively. The bands monitored for VET experiments are indicated by arrows in the spectra.

to vary according to the zero-order quantum description of the initially pumped level. This initial state sensitivity persists even for the highest state densities. The quoted vibrational state densities in CCP and the present work were obtained by a harmonic direct count algorithm using S_1 pDFB frequencies where available and S_0 frequencies reduced by the average S_1/S_0 ratio of known frequencies otherwise.[29]

The primary results of the present study are rate constants for three new initial states of S_1 pDFB at still higher vibrational energies where the state densities lie in the range 800−2000 per cm^{-1}. These data are reported in Table 1 for the collision partners He and Ar. Additionally, the Table includes remeasurement of Ar rate constants for some of the lower energy initial levels previously studied[4] plus entirely new measurements of He rate constants for many lower levels.

Anticipated Relaxation Characteristics of Highly Excited Molecules. One of the questions relevant to interpretation of these results concerns the extent to which these higher pDFB levels replicate characteristics of the levels involved at the high vibrational energies of the unimolecular activation/deactivation problem. Consider first the extent to which the vibrational quasi-continuum associated with activated molecules might be replicated. The S_1 pDFB lifetimes are approximately 5 ns[26] corresponding to vibrational level widths of about 1×10^{-3} cm^{-1}. Thus level overlap will just begin to occur where the previous data ended at pDFB vibrational densities of approximately 200 per cm^{-1}. Our new data extend to regions with about 2000 states per cm^{-1} where a quasi-continuum is probably beginning to appear.

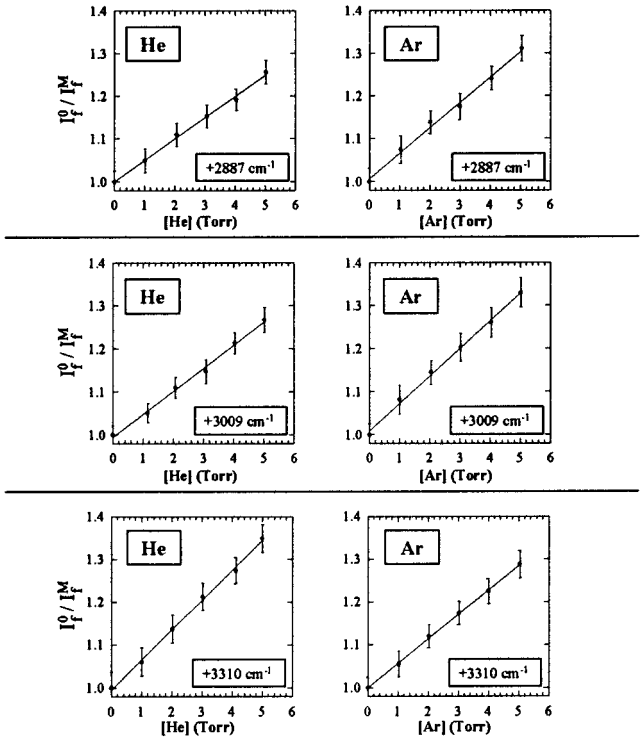

Figure 3. Stern−Volmer plots of fluorescence intensity in the monitored bands for the three highest levels that are being destroyed by state-to-field VET in collisions with He and Ar.

A second vibrational characteristic concerns the quantum description of the vibrational manifold. No matter how one might describe the states of an activated molecule with high vibrational excitation, these regions must involve vibrational states that are highly mixed in a zero-order basis. None will be dominated by the character of a single zero-order quantum state. Ironically, to reach analogous states in S_1 pDFB, our experiments must rely on the character of a single zero-order state that has a large S_1-S_0 Franck−Condon factor to provide access to an S_1 vibrational region.[30] For example, as described with zero-order vibrational components, our three newly studied higher energy regions are pumped using the Franck−Condon factors for the $3_0^1 5_0^2$, $3_0^1 5_0^2 30_1^1$ and $3_0^2 5_0^1$ transitions.[31] Despite such Franck−Condon bias in S_1 level pumping, this character is diluted among the set of molecular eigenstates actually pumped in the S_1-S_0 transition. While each molecular eigenstate is a mixture of many zero-order states, every pumped eigenstate has a small component of the Franck−Condon state. For this reason, the Franck−Condon state appears prominently in the absorption spectrum and is a useful zero-order description.[30]

Most importantly, each of the eigenstates encountered by the collision partner is broadly mixed. A full discussion of their character is given elsewhere.[30,4] The evidence for the mixed character lies in the collision free fluorescence spectra from these levels. That emission is dominated by unstructured fluorescence with only a vestige of structure from the Franck−Condon component. Such emission is characteristic of fluorescence from vibrational states with extensive mixing among zero-order vibrational states.[32]

In the regions previously studied, the rate constants gradually increase with rising vibrational energy, but that trend is overlaid

TABLE 1: Experimental Rate Constants k_4 and Cross Sections σ_v for State-to-Field Vibrational Energy Transfer from Initial S_1 Levels of pDFB in Collision with Ar and He at 300 K

initial level	E_{vib} (cm^{-1})	τ_f (ns)[a]	k_4 (10^7 Torr^{-1} s^{-1})[b]		k_4/k_{HS}[c]		k_4/k_{LJ}[d]		σ_v (Å^2)[e]	
			He	Ar	He	Ar	He	Ar	He	Ar
5^1	818	10.0	0.23 ± 0.02	0.33 ± 0.03	0.08	0.26	0.08	0.19	5.60	22.2
3^1	1251	9.7	0.47 ± 0.04	0.53 ± 0.04	0.16	0.42	0.16	0.30	11.4	35.6
5^2	1638	8.6	0.55 ± 0.08	0.76 ± 0.04	0.19	0.60	0.19	0.43	13.4	51.1
3^15^1	2069	7.8	0.61 ± 0.04	1.26 ± 0.04	0.21	0.99	0.21	0.72	14.9	84.8
5^3	2454	6.5	0.64 ± 0.04	0.94 ± 0.04	0.22	0.74	0.22	0.54	15.6	63.3
3^2	2502	6.3	1.40 ± 0.04	1.50 ± 0.03	0.47	1.18	0.49	0.86	34.1	101.0
3^15^2	2887	6.5	0.81 ± 0.04	0.97 ± 0.04	0.27	0.76	0.28	0.55	19.7	65.3
$3^15^230^1$	3009	6.5[f]	0.82 ± 0.05	0.98 ± 0.05	0.28	0.77	0.29	0.56	20.0	66.0
3^25^1	3310	5.7	1.10 ± 0.03	1.00 ± 0.03	0.37	0.79	0.38	0.57	26.8	67.3

[a] Values obtained by Guttman and Rice.[26] [b] For conversion to cm^3 molecule^{-1} s^{-1}, multiply by 3.1×10^{-17}. [c] $k_{HS} = (8kT/\pi\mu)^{1/2}\sigma_{HS}$, where $\sigma_{HS} = (\pi/4)(d_{pDFB} + d_M)^2$, $d_{pDFB} = 7.0$ Å, $d_{He} = 2.57$ Å, and $d_{Ar} = 3.41$ Å.[3] [d] $k_{LJ}(He) = 2.87 \times 10^7$ Torr^{-1} s^{-1}, $k_{LJ}(Ar) = 1.75 \times 10^7$ Torr^{-1} s^{-1}.[3] [e] $\sigma_v = k_4/(8kT/\pi\mu)^{1/2}$. [f] *Assumed* lifetime is equal to that of the 3^15^2 level lying 122 cm^{-1} lower in energy.

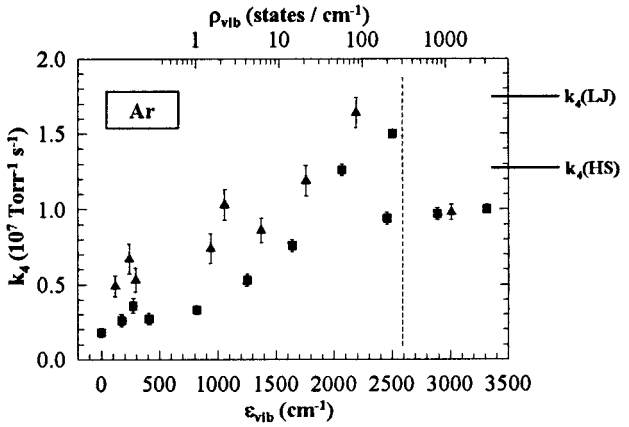

Figure 4. Plot of measured k_4 values against the energy ϵ_{vib} and state density ρ_{vib} of the pumped level for deactivation of pDFB by Ar. Levels with quanta of ν_{30} are indicated as triangle symbols. The hard sphere and Lennard-Jones rate constant values are indicated by markers at the right of the figure. A dashed line indicates the highest energy region studied by CPP.

with a large sensitivity to the zero order description of the initially pumped vibrational state. Modeling[2,4] shows that the trend to larger rate constants is a consequence of the fact that more channels contribute to VET at higher vibrational energy, each with small state-to-state transition probability. The modeling also shows that the rate constant sensitivity to the initially pumped state is due to special channels that are so favored for some initial states that they alone make a significant contribution to the total rate constant.

From these concepts, one can now generate two expectations for the rate constants as VET is probed from regions of increasingly higher vibrational energy. First, the extensive state mixing will ultimately so dilute individual state character that sensitivity to the pumped zero-order state will damp out. Second, the slow response to increasing state densities as higher initial levels are pumped cannot go on forever. The rate constants will ultimately level off somewhere after the vibrational quasi-continuum has become well established. One might propose that such characteristics are also representative of the rate constants in the VET activation/deactivation process of unimolecular reactions.

Rate Constants for Ar + pDFB. We now examine the data relative to these expectations using the display of rate constants for Ar against ϵ_{vib} or ρ_{vib} in Figure 4. The data for levels up to $\epsilon_{vib} = 2502$ cm^{-1} are as described before. The high sensitivity to the quantum identity of the initially pumped level and the rising trend with increasing ϵ_{vib} are confirmed by our new measurements in this previously studied region.

The measurements of VET from the three higher energy levels (2887 cm^{-1} $\leq \epsilon_{vib} \leq$ 3310 cm^{-1}) with densities ranging from approximately 800 to 2000 states per cm^{-1} produce rate constants that are essentially the same. The constants respond neither to increasing state density nor to the quantum state identity of the initially pumped level.

The S_1 levels of pDFB provide a good opportunity to search for sensitivity of state-to-field VET to the quantum identity of the pumped state. Levels accessible for study include those related to each other by the absence or presence of a quantum of the lowest frequency mode $\nu_{30}' = 120$ cm^{-1}. Eight such pairs are represented in the lower energy region ($\epsilon_{vib} < 2300$ cm^{-1}) of the rate constants shown in Figure 4. For each pair, the rate constant for the level containing a quantum of ν_{30}' is enhanced on account of the $\Delta v_{30} = -1$ state-to-state channel that is available only to the level containing a ν_{30}' quantum.[4] That channel has been well characterized[33] as the largest among the many state-to-state channels monitored in S_1 pDFB. It has been observed from many different initial levels, and always occurs with about the same rate constant, approximately $k = 0.26 \times 10^7$ Torr^{-1} s^{-1} (12 Å^2 cross section). This channel is so favored that its presence may increase the state-to-field rate constant by more than fifty percent.

The new higher energy region explored in the present study contains a pair of levels similarly related. That pair provides a test for whether quantum state sensitivity persists at these higher state densities. The states are 3^15^2 (at 2887 cm^{-1}) and $3^15^230^1$ (at 3009 cm^{-1}). The Ar rate constants for this pair are almost identical, and in this respect, they are qualitatively different from those of all other pairs. By the example of these data, the quantum state sensitivity has been lost.

With quantum state sensitivity damped out at the highest energies of this study, one might contemplate whether the rate constants are actually approaching a limiting value. Obviously data from higher levels are needed to secure the issue. If, however, a limiting value is indeed beginning to emerge, it is interesting to note that the value is substantially less than that of rate constants for energy transfer from several lower energy levels that display strong quantum state sensitivity. The reason for this behavior is not understood.

Rate Constants for He + pDFB. In some respects, the He data in Figure 5 mirror the Ar results. As with Ar, the He rate constants show a trend to larger values for initial levels with higher energy. The He rate constants have also maintained sensitivity to the quantum character of the initially pumped state, at least for the lower levels. The most convincing example of this sensitivity for He concerns the initial levels 5^3 and 3^2. Lying

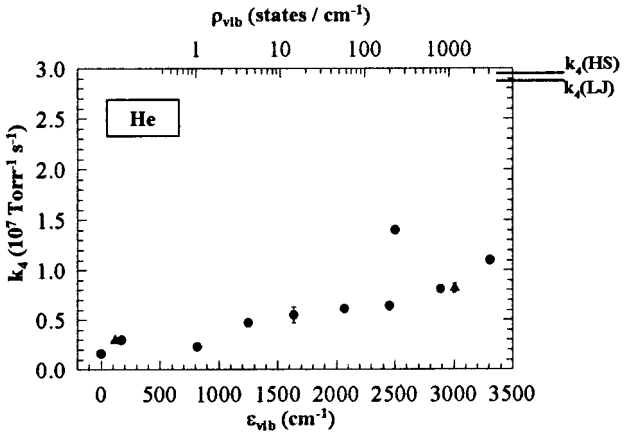

Figure 5. Plot of measured k_4 values against the energy ϵ_{vib} and state density ρ_{vib} of the pumped level for deactivation of pDFB by He. Levels with quanta of ν_{30} are indicated as triangle symbols. The hard sphere and Lennard-Jones rate constant values are indicated by markers at the right of the figure.

near $\epsilon_{vib} = 2500$ cm^{-1}, they are separated by only about 50 cm^{-1} but have rate constants differing by about a factor of 2.

The principal question is whether the rate constants give signs of replicating the proposed behavior of highly excited levels as the initial vibrational excitation becomes greater. In this respect, He behavior differs from that of Ar. One cannot argue that the trend toward larger rate constants has leveled off for the higher vibrational state densities, nor can a case be made for the disappearance of quantum state sensitivity at high energies, although the data are ambiguous on this point. As discussed above for Ar collisions, the pair of levels pumped near 3000 cm^{-1} ($\rho_{vib} \approx 800$ per cm^{-1}) provides a test since their zero order assignments differ only by a quantum of ν_{30}'. Even though the rate constants for this pair are the same, the rate constant for the next higher level at $\epsilon_{vib} = 3310$ cm^{-1} ($\rho_{vib} \approx 2000$ per cm^{-1}) is substantially larger. There is no way to know from the present data whether the increase is due to initial quantum state sensitivity or to the increased vibrational state density or both.

The differing behaviors of He vs Ar as a VET collision partner for S_1 pDFB has been seen also in an earlier state-to-state study.[27] Modeling[27] of the state-to-state VET with SSH-T theory[34,35] suggests that the unique behavior of each gas is a consequence of differences in their reduced masses (i.e., a kinematic effect) and, to a lesser extent, their intermolecular potential well depths.

Comparisons with Lennard-Jones and Hard Sphere Rate Constants. The plots of Ar and He rate constants in Figures 4 and 5 contain markers for the size of Lennard-Jones and hard sphere rate constants. The Lennard-Jones and hard sphere values for He collisions are almost the same but unusual in that the hard sphere rate constant is the larger. The data in Figure 5 show that the largest He rate constants are less than half of the Lennard-Jones value. The trend to larger rate constants with higher ϵ_{vib} is moving so slowly that it appears unlikely that He rate constants would ever reach these benchmarks.

Several of the Ar rate constants in Figure 4 match or exceed the hard sphere value, and one comes close to the Lennard-Jones value. These large values occur only for ϵ_{vib} regions where a strong response to quantum state identity persists. For the highest ϵ_{vib} regions where this quantum state sensitivity appears to have been damped out, the rate constants have leveled off near the hard sphere value and are well below the Lennard-Jones rate constants.

SO_2 Rate Constants. Xue, Han and Dai[28] have reported absolute rate constants for collisional destruction of highly excited SO_2 by He, Ar and unexcited SO_2. The excited level is a single rovibronic level lying at 44 878 cm^{-1} in the $\tilde{X}$ state. The level can be detected due to the fact that it is mixed with an isoenergetic $\tilde{C}$ rovibrational level that is reached by pumping the $^qR(6)_{1,5}$ line in the $1_0^2 2_0^1 3_1^0$ band of the $\tilde{C} \leftarrow \tilde{X}$ transition. The strong coupling of these levels generates quantum beats in the $\tilde{C} \rightarrow \tilde{X}$ fluorescence. The quantum beat decay is sensitive to added gas or SO_2 pressure, and the rate constant for collisional destruction of the rovibronic eigenstate high in the $\tilde{X}$ state manifold can be extracted from that sensitivity.

The SO_2 rate constants are much larger than those for the highest levels of the present pDFB study. For this highly excited SO_2 molecule, the rate constants exceed Lennard-Jones values for the three collision partners He, Ar and unexcited SO_2 by factors of 2.6, 3.6 and 11, respectively. In contrast, the state-to-field rate constants for the highest levels of S_1 pDFB interacting with He or Ar are only about 40% and 60%, respectively, of the Lennard-Jones value. (For comparison, the $SO_2{}^{*-}$ Ar rate constant is 3.7×10^7 Torr^{-1} s^{-1} vs the apparent pDFB*-Ar limiting value of approximately 1×10^7 Torr^{-1} s^{-1}.) It is hard to see from the pDFB trends that the state-to-field rate constants would ever become similar to the SO_2 magnitudes as the pDFB vibrational excitation increased. Thus the two molecules appear as complementary systems with fundamentally different behaviors for collisional deactivation. One is a small molecule with very high vibrational excitation but a sparse level structure. The vibrational level density is on the order of one per cm^{-1}. The large molecule, on the other hand, has modest vibrational energy but with the vibrational level structure of a quasi-continuum.

While it is not possible to secure the underlying causes of the different rate constants for these systems, two aspects that might contribute to the large SO_2 rate constants have been discussed.[28] One is related to the nature of the SO_2 experiments themselves and one is a fundamental property of excited SO_2 itself. Neither can contribute to the pDFB rate constants.

The first concerns the fact that the SO_2 experiments necessarily monitor the destruction of a single rovibronic eigenstate. Rotational energy transfer will appear as state destruction and, along with vibrational relaxation, contribute to the observed rate constant. What the relative magnitudes of these two relaxation channels so high in the $\tilde{X}$ manifold will be is not clear. In this respect, the pDFB system is intrinsically more accommodating. As is done in the present work, it is relatively easy to make the pDFB observations blind to rotational relaxation so that the rate constants are solely those of vibrational relaxation.

The second concerns the strong vibronic coupling between the $\tilde{X}$ and $\tilde{C}$ states of SO_2. This coupling can provide enhanced vibrational energy transfer by allowing the $\tilde{C}-\tilde{X}$ electronic transition dipole moment to contribute by long-range interactions to the matrix elements responsible for V−T,R energy transfer involving levels in the $\tilde{X}$ state. The mechanism has been discussed in connection to collisional relaxation studies in NO_2,[13,36] CS_2[13,36] and in SO_2[28,37,38] itself. Studies for each triatomic molecule used time-resolved FTIR emission spectroscopy to monitor the average energy loss per collision $\langle \Delta E \rangle$ as a function of the initial energy $\langle E \rangle$. For all three molecules, $\langle \Delta E \rangle$ is enhanced as $\langle E \rangle$ climbs above a threshold value. Analogous behavior occurs in excited pyrazine[22] for which the V−T,R energy transfer characteristics in CO_2 collisions change suddenly as the pyrazine internal energy climbs above 36000 cm^{-1}. In the cases of NO_2 and CS_2, the threshold corresponds to the position of an observed excited electronic state to which strong

vibronic coupling occurs. An S_2 state is known to be near the pyrazine threshold.

Contributions to the pDFB vibrational energy transfer rate constant from long-range dispersion force interactions involving the electronic transition dipole, in this case the S_1-S_0 transition dipole, seem unimportant. The evidence lies in the close match of vibrational energy transfer rate constants for the S_0[3,5] and S_1[4] states when regions of similar vibrational state density are compared.

While strong vibronic coupling is not among the S_1 interactions of pDFB, weak vibronic interactions of S_1 pDFB with the S_0 and the T_1 states are certainly present. In this context, it is instructive to note that an examination of the role of S_1-T_1 vibronic coupling on vibrational relaxation in large molecules has been presented.[39] Ironically, when these couplings influence the S_1 vibrational relaxation, they are expected to reduce rather than enhance the observed rate constants. VET in S_1 pyrimidine is a example of this effect. As far as can be determined presently, the weak vibronic interactions of S_1 pDFB do not substantially influence the S_1 vibrational energy transfer.

Conclusions

Absolute rate constants have been measured for state-to-field vibrational relaxation of S_1 pDFB levels in single-collisions with Ar or He. For Ar collisions, the measurements build on earlier values reported for the region $0 \leq \epsilon_{vib} \leq 2502$ cm^{-1}. New rate constants for three higher levels ($2887 \leq \epsilon_{vib} \leq 3310$ cm^{-1}) extend the data to regions where the state densities range from about 800 per cm^{-1} to 2000 per cm^{-1} and the level structure is probably that of a quasi-continuum. The He measurements span the entire range from the zero point level to the highest level of the Ar data.

The primary question centers on the observed rate constants at the higher energies. Have they acquired the characteristics that one might expect for the vibrational activation/deactivation of molecules with the high excitation of unimolecular reaction systems? Do they approach the values of the Lennard-Jones rate constants usually adopted for models of unimolecular reaction activation/deactivation?

The Ar rate constants for the three highest energy levels have the expected unimolecular behavior. Consistent with the highly mixed vibrational character of levels in the quasi-continuum, they are not sensitive to the zero-order normal mode descriptions used for the optical pumping. Additionally, the rate constants for these regions appear to have leveled off after the trend to larger values for lower levels of increasing vibrational energy.

Different techniques must be used to extend the study to higher vibrational regions in order to learn whether these characteristics persist as the vibrational quasi-continuum becomes more dense. If indeed a limit has been reached in the present Ar experiments, the rate constants provide insight to the question of whether Lennard-Jones rate constants are appropriate for unimolecular modeling. The high energy level rate constants are only about 60% of the Lennard-Jones benchmark.

The situation for He collisions differs. The rate constants appear to sustain a trend to larger values with increasing vibrational energy even in the highest energy regions where the Ar rate constants have leveled off. The data are ambiguous on whether initial quantum state sensitivity persists at the highest energies. In addition to indications that He rate constants never fully display the predicted unimolecular activation/deactivation behavior, they are also well below the Lennard-Jones benchmark. The largest rate constants are only 30−40% of the Lennard-Jones value.

Acknowledgment. We are grateful for the financial support of the National Science Foundation. Discussions with Professor H. L. Dai and Mr. Uros Tasic have been helpful.

References and Notes

(1) Logan, L. M.; Buduls, I.; Knight, A. E. W.; Ross, I. G. *J. Chem. Phys.* **1980**, *72*, 5667.
(2) Tang, K. Y.; Parmenter, C. S. *J. Chem. Phys.* **1983**, *78*, 3922.
(3) Kable, S. H.; Thoman, J. W., Jr.; Knight, A. E. W. *J. Chem. Phys.* **1988**, *88*, 4748.
(4) Catlett, D. L., Jr.; Parmenter, C. S.; Pursell, C. J. *J. Phys. Chem.* **1995**, *99*, 7371.
(5) Thoman, J. W., Jr.; Kable, S. H.; Rock, A. B.; Knight, A. E. W. *J. Chem. Phys.* **1986**, *85*, 6234.
(6) Tardy, D. C.; Rabinovitch, B. S. *Chem. Rev.* **1977**, *77*, 369.
(7) Oref, I.; Tardy, D. C. *Chem. Rev.* **1990**, *90*, 1407.
(8) Quack, M.; Troe, J. *Int. Rev. Phys. Chem.* **1981**, *1*, 97.
(9) Weston, R. E., Jr.; Flynn, G. W. *Annu. Rev. Phys. Chem.* **1992**, *43*, 559.
(10) Barker, J. R.; Toselli, B. M. *Int. Rev. Phys. Chem.* **1993**, *12*, 305.
(11) Flynn, G. W.; Parmenter, C. S.; Wodtke, A. M. *J. Phys. Chem.* **1996**, *100*, 12817.
(12) Barker, J. R. *J. Phys. Chem.* **1985**, *88*, 11.
(13) Hartland, G. V.; Qin, D.; Dai, H. L.; Chen, C. *J. Chem. Phys.* **1997**, *107*, 2890.
(14) Troe, J. *J. Chem. Phys.* **1977**, *66*, 4758.
(15) Lenzer, T.; Luther, K.; Troe, J.; Gilbert, R. G.; Lim, K. F. *J. Chem. Phys.* **1995**, *103*, 626.
(16) Wright, S. M. A.; Sims, I. R.; Smith, I. W. M. *J. Phys. Chem. A* **2000**, *104*, 10347.
(17) Damm, M.; Hippler, H.; Troe, J. *J. Chem. Phys.* **1988**, *88*, 3564.
(18) Bernshtein, V.; Oref, I. *J. Chem. Phys.* **1998**, *108*, 3543.
(19) Hold, U.; Lenzer, T.; Luther, K.; Reihs, K.; Symonds, A. *Ber. Bunsen-Ges. Phys. Chem.* **1997**, *101*, 552.
(20) Sevy, E. T.; Michaels, C. A.; Tapalian, H. C.; Flynn, G. W. *J. Chem. Phys.* **2000**, *112*, 5844.
(21) Lenzer, T.; Luther, K. *J. Chem. Phys.* **1996**, *105*, 10944.
(22) Elioff, M. S.; Wall, M. C.; Mullin, A. S. *J. Chem. Phys.* **1999**, *110*, 5578.
(23) Abel, B.; Lange, N.; Reiche, F.; Troe, J. *J. Chem. Phys.* **1999**, *110*, 1389.
(24) Abel, B.; Lange, N.; Reiche, F.; Troe, J. *J. Chem. Phys.* **1999**, *110*, 1404.
(25) Bevilacqua, T. J.; Weisman, R. B. *J. Chem. Phys.* **1993**, *98*, 6316.
(26) Guttman, C.; Rice, S. A. *J. Chem. Phys.* **1974**, *61*, 661.
(27) Catlett, D. L., Jr.; Parmenter, C. S. *J. Phys. Chem.* **1991**, *95*, 2864.
(28) Xue, B.; Han, J.; Dai, H. L. *Phys. Rev. Lett.* **2000**, *84*, 2606.
(29) Catlett, D. L., Jr. Vibrational energy flow in the S_1 ($^1B_{2u}$) state of *p*-difluorobenzene. Ph.D. Thesis, Indiana University, 1985.
(30) Holtzclaw, K. W.; Parmenter, C. S. *J. Chem. Phys.* **1986**, *84*, 1099.
(31) Coveleskie, R. A.; Parmenter, C. S. *J. Mol. Spectrosc.* **1981**, *86*, 86.
(32) Dolson, D. A.; Holtzclaw, K. W.; Moss, D. B.; Parmenter, C. S. *J. Chem. Phys.* **1986**, *84*, 1119.
(33) Catlett, D. L., Jr.; Parmenter, C. S.; Pursell, C. J. *J. Phys. Chem.* **1994**, *98*, 3263.
(34) Schwartz, R. N.; Slawsky, Z. I.; Herzfeld, K. F. *J. Chem. Phys.* **1952**, *20*, 1591.
(35) Tanczos, F. I. *J. Chem. Phys.* **1956**, *25*, 439.
(36) Hartland, G. V.; Qin, D.; Dai, H. L. *J. Chem. Phys.* **1995**, *102*, 8677.
(37) Qin, D.; Hartland, G. V.; Chen, C. L.; Dai, H. L. *Z. f. Phys. Chem.* **2000**, *214*, 1501.
(38) Qin, D.; Hartland, G. V.; Dai, H. L. *J. Phys. Chem. A* **2000**, *104*, 10460.
(39) Knight, A. E. W.; Parmenter, C. S. *J. Phys. Chem.* **1983**, *87*, 417.